NASA CONTRACTOR REPORT

NASA CR-61195

February 1968

NASA CR-61195

GPO PRICE $ _____

CFSTI PRICE(S) $ _____

Hard copy (HC) 3.00

Microfiche (MF) .65

ff 653 July 65

MATHEMATICAL WIND PROFILES

Prepared under Contract No. NAS 8-5380 by
Arnold Court, Robert R. Read and Gerald E. Abrahms

LOCKHEED-CALIFORNIA COMPANY

For

NASA-GEORGE C. MARSHALL SPACE FLIGHT CENTER
Huntsville, Alabama

February 1968 NASA CR-61195

MATHEMATICAL WIND PROFILES

By

Arnold Court, Robert R. Read and
Gerald E. Abrahms

Prepared under Contract No. NAS 8-5380 by

LOCKHEED-CALIFORNIA COMPANY

For

Aero-Astrodynamics Laboratory

NASA-GEORGE C. MARSHALL SPACE FLIGHT CENTER

MATHEMATICAL WIND PROFILES[1]

By

Arnold Court, Robert R. Read,[2] and Gerald E. Abrahms

Office of the Chief Scientist
Lockheed-California Co.
Burbank, California

ABSTRACT

Augmented Fourier polynomials, in which constant and linear terms have been added to a complex Fourier series, appear to offer a means for representing the vertical profile of the horizontal wind velocity. Reasons for selecting this function, and methods of its computation and application, are given. Polynomial coefficients are presented for mean monthly winds over Cape Kennedy, Florida, and for four consecutive soundings over Montgomery, Alabama.

---

1 Prepared under Contract NAS-8-5380 with Aero-Astrodynamics Laboratory, George C. Marshall Space Flight Center, NASA, with O. E. Smith as Technical Supervisor. Arnold Court and Gerald E. Abrahms, are Senior Scientists, affiliated with the Lockheed-California Company.

2 Associate Professor of Mathematics, U. S. Navy Postgraduate School, Monterey, and Consultant to the Lockheed-California Company.

NASA - GEORGE C. MARSHALL SPACE FLIGHT CENTER

MATHEMATICAL WIND PROFILES

SUMMARY

Augmented Fourier polynomials, in which constant and linear terms have been added to a complex Fourier series, appear to offer a means for representing the vertical profile of the horizontal wind velocity. Reasons for selecting this function, and methods of its computation and application, are given. Polynomial coefficients are presented for mean monthly winds over Cape Kennedy, Florida, and for four consecutive soundings over Montgomery, Alabama.

1. Introduction

Mathematical representation of the vertical profile of wind is desirable for many purposes, and essential for the rigorous comparison of profiles and the prediction of profiles by statistical regression techniques. Because wind is a two-dimensional vector (neglecting the vertical component, which is at least an order of magnitude smaller than the horizontal components), the vertical profile of the instantaneous wind is a curve in three-dimensional space. The graphical and analytical difficulties in describing such a curve have thus far prevented any systematic description of complete wind profiles. In this report, various possible methods of representation are explored, and one of them, using complex Fourier series, is developed in detail. Application of the method, and its evaluation, will be the subjects of future reports.

Notation has been chosen carefully for consistency and clarity. The wind speed toward the east is denoted by x, that toward the north by y. Their vector resultant is called $\underline{z}$, and the modulus or absolute value of the resultant is z:

$$|\underline{z}|^2 = z^2 = x^2 + y^2. \tag{1.1}$$

The direction of this resultant, in degrees clockwise from north, is

$$\theta = \text{arc sin } \frac{x}{z} = \text{arc cos } \frac{y}{z} . \tag{1.2}$$

This double definition eliminates the ambiguity of sign inherent in a definition based on arc tan y/x. The meteorological convention for angles, used also in surveying and navigation, differs from the mathematical practice, in which angles are measured counterclockwise from the x-axis (east in meteorological practice). For the mathematical development, therefore, the direction is designated as

$$\phi = \frac{\pi}{2} - \theta = \text{arc sin } \frac{y}{z} = \text{arc cos } \frac{x}{z}, \tag{1.3}$$

and hence measured counterclockwise from east.

Alternative to the Cartesian (x, y), polar (z, θ), and vector ($\underline{z}$) representations of a wind vector is its representation as a complex variable, ζ:

$$\zeta = \underline{z} = x + i\,y = ze^{i\phi}. \tag{1.4}$$

To reduce the number of subscripts, a second wind vector will be denoted as (u, v), (w, ψ), $\underline{w}$, or $\eta = w \exp(i\xi)$. Height upward from the ground will be designated as h, atmospheric density as q, true correlation as ρ and its sample estimate as r, true variance as σ^2 and its sample estimate as s^2, and gravity as g.

The complex conjugate of a complex number will be denoted by an asterisk:

$$\zeta^* = x - iy = ze^{-i\phi}. \tag{1.5}$$

Therefore, the real and imaginary parts of the complex number ζ are

$$\begin{aligned} \tilde{\tilde{R}}(\zeta) &= \frac{\zeta + \zeta^*}{2} = z\,\frac{e^{i\phi} + e^{-i\phi}}{2} = z \cos\phi = x, \\ \tilde{\tilde{C}}(\zeta) &= \frac{\zeta - \zeta^*}{2} = z\,\frac{e^{i\phi} - e^{-i\phi}}{2} = z \sin\phi = y. \end{aligned} \tag{1.6}$$

Other notation will be identified when used.

2. Representations

Because a wind profile is a curve in three-dimensional space, its graphical representation on two-dimensional paper requires elimination of one dimension. Various graphical methods have been used for many years, each with some advantages and many disadvantages. The four basic methods, illustrated in Figure 1 with mean January winds for Cape Kennedy, Florida, are

a. each component, separately, vs height

b. speed and direction, separately, vs height

c. velocity hodograph

d. position hodograph.

The first two methods require mental addition of values from the two lines to give a picture of the actual wind vector and its changes. This difficulty is eliminated in the hodographs, in which the vertical dimension (or time) is indicated only by successive points along the path.

A hodograph is a curve connecting the end-points of successive vectors drawn from a common origin. The vectors may be successive in height, to represent the wind profile, or in time, to show the time variation of wind. The former application is used here, but the mathematical formulation is equally applicable to the time series case. The vectors may represent the actual wind velocity at each level, or they may represent the integral of the velocity, which gives the position of an object, such as a balloon, rising with constant speed through the wind field. The usual plotting-board representation of a pilot balloon trajectory is a position hodograph of the vertical wind profile, while the similarity trajectory of a constant-level balloon is a position hodograph of the time variation of wind. A position hodograph can be prepared from wind velocity information by plotting the successive vectors additively rather than from a common origin.

Hodographs appear more suitable for mathematical representation of the vertical wind profile than separate representations by components, or by speed and direction. But choice between the two hodographs, velocity and position, is more difficult. Fortunately, the computational procedures of fitting a function to observations are the same for either type of hodograph, since the purpose is merely to obtain an analytic function describing the curve.

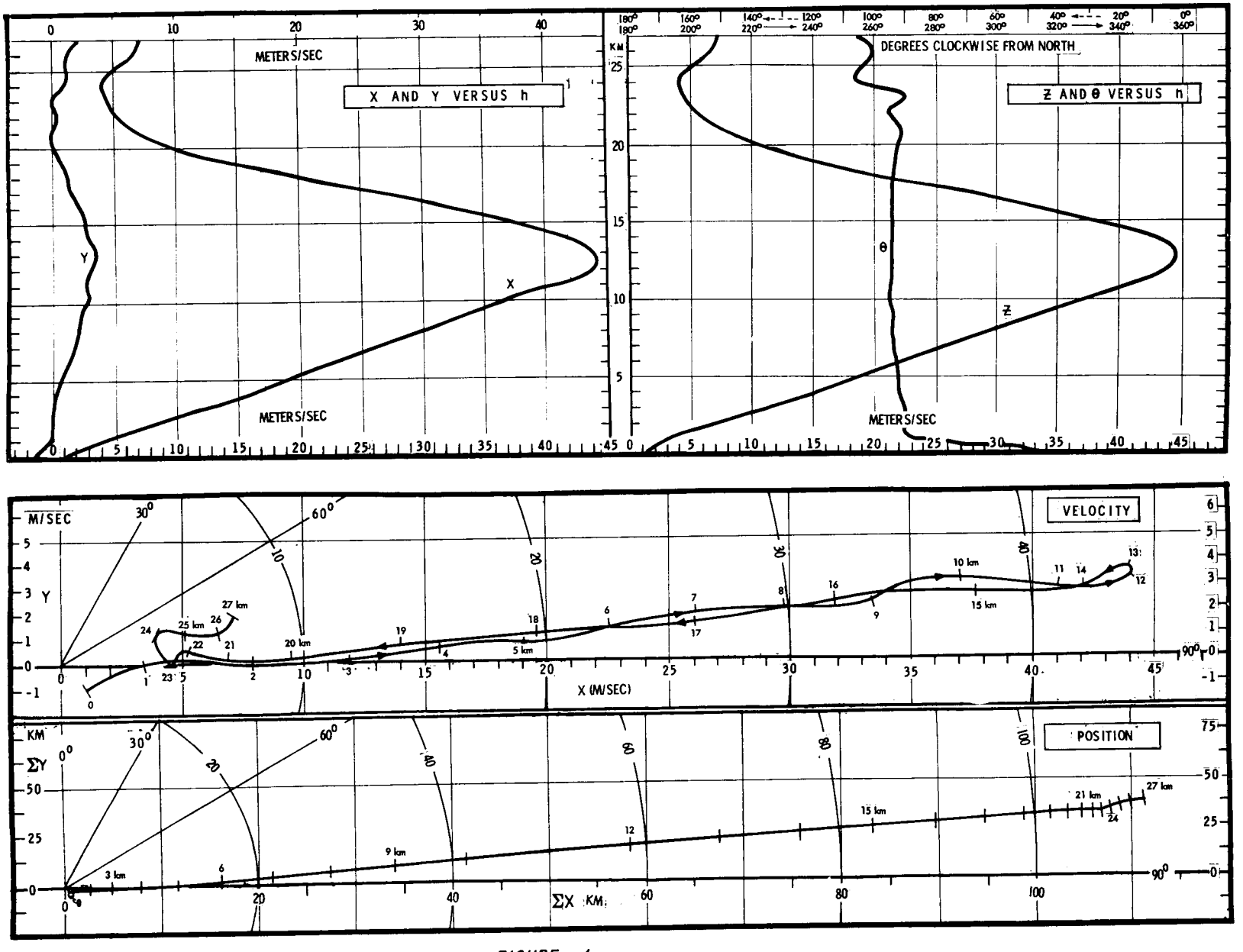
METERS/SEC
X AND Y VERSUS h
Y
X
METERS/SEC
DEGREES CLOCKWISE FROM NORTH
Ż AND θ VERSUS h
θ
Ż
METERS/SEC
KM
M/SEC
VELOCITY
X (M/SEC)
KM
ΣY
POSITION
ΣX KM

FIGURE 1

When positions actually are measured (as in most meteorological observations using balloons, rising or falling), the position hodograph should be fitted. One differentiation of the fitted function then will give the velocity hodograph function, and a second differentiation the wind shear, which is of considerable importance. Actually, most routine wind information is obtained from finite differences of balloon positions, and shears from finite differences of these computed velocities, i.e., by smoothed second differences of the basic observations.

When wind velocities are obtained directly, as by sound ranging, the velocity hodograph should be fitted. One differentiation then will yield shears, while integration gives the positions to which they apply. Such positional information is needed for studies of the trajectories of falling or suspended objects, such as radioactive fallout or toxic pollutants.

Any mathematical function used to approximate a hodograph must be continuous and have continuous first and second derivatives. Since the hodograph is a vector-valued function $\underline{z}(h)$ of a scalar argument, h, in practice, representation by components is more convenient. Compactness of representation and relative ease of manipulation make the complex form,

$$x(h) + iy(h), \qquad z(h) \exp [i\phi(h)],$$

suited for an attempt at developing an expression for $\underline{z}(h)$.

3. Functions

Selection of a mathematical function to approximate the vertical wind profile, as represented by its position or velocity hodograph, must be based largely on convenience and general suitability, including possession of continuous derivatives. Meteorological theory and hydrodynamic theory are as yet inadequate to provide a definitive functional form, except for certain height ranges.

In the lowermost ten meters of the atmosphere, air flow increases with height without material change in direction (Hess, 1959) [2]. When the temperature lapse rate is neutral, the logarithmic wind profile appears to fit available observations:

$$z = \frac{\sqrt{\tau/\varrho}}{k} \ln \frac{h}{h_o} \tag{3.1}$$

where τ is the eddy stress, q the density, k von Karman's constant, and h_o a "roughness parameter." When the lapse rate is not neutral, an exponential profile seems more appropriate:

$$z = z_1(h/h_1)^m \tag{3.2}$$

where z_1 is the wind speed at height h_1 (usually a few centimeters) and m is a positive exponent less than unity. A generalization, for variable lapse rates, is offered by the Deacon profile:

$$z = \left[\frac{\sqrt{\tau/q}}{k(1 - \beta)}\right]\left[\left(\frac{h}{h_o}\right)^{1-\beta} - 1\right]. \tag{3.3}$$

For several hundred meters above this boundary layer, wind increases in speed with height, and turns clockwise, in the northern hemisphere, generally according to the Ekman spiral. At about the 10-meter level, the wind is directed toward the left of the geostrophic wind, which blows along the isobars at 1 km or higher. The wind vector at height h in this spiral or friction layer is

$$z(h) = z_g\left[e^{i\phi} - e^{-ah}\, e^{i(ah-\phi)}\right]. \tag{3.4}$$

Here z_g is the magnitude of the geostrophic wind, blowing at an angle ϕ (in mathematical notation) to the positive x-axis, and a is a function of density, Coriolis force, and eddy viscosity. Actual winds do follow this Ekman spiral when the upper wind flow is straight or only slightly curved, and the lowermost kilometer of air has no appreciable horizontal gradients of temperature.

Above the spiral layer, wind speed generally increases with height up to the level of maximum wind, which usually occurs slightly below the tropopause at 10 to 12 km. Often the increase in speed with height is at about the same rate as the decrease of density with height, so that between 5 and 10 km "Egnell's law" states that the momentum is constant. A justification of this empirical rule, deduced from cloud and pilot balloon observations 70 years ago by Clayton in Massachusetts and Egnell in France, was offered by Humphreys (1929, pp. 135-136) [1].

Above the maximum wind layer, wind speed decreases with height to a minimum, on the average, at 22 to 25 km, but no law or rule describing this decrease, or the accompanying change in direction, has yet appeared. Thus, while some theoretical formulations are available for wind behavior in the boundary and spiral layers, a few guidelines can be found for the form of a function to describe the wind profile above 1 km.

4. Series

In the absence of any theory on which to base a functional form for wind profile description, some empirical function must be chosen. Logical candidates for this purpose are polynomials. The wind vector $\underline{z} = (x, y)$ could be represented as a function of height, h, by two separate polynomials, one for each component:

$$x_{h,m} = \sum_{k=0}^{m} a_k h^k, \qquad y_{h,n} = \sum_{k=0}^{n} b_k h^k \tag{4.1}$$

where m and n are the numbers of terms required for satisfactory fit or agreement of the polynomial with the observations. Agreement would be determined by the variance (mean squared difference) of the observations about the polynomials. The absolute or unconditional variances are, respectively, s_x^2 and s_y^2, and the conditional variances $s_{x,m}^2$ and $s_{y,n}^2$:

$$s_x^2 = \nu^{-1} \sum (x_h - \bar{x})^2 = \nu^{-1} \sum x_h^2 - (\bar{x})^2,$$

$$s_{x,m}^2 = \nu^{-1} \sum (x_h - x_{h,m})^2 = \nu^{-1} \sum x_h^2 + \nu^{-1} \sum x_{h,m}(x_{h,m} - 2x_h), \tag{4.2}$$

and similarly for s_y^2 and $s_{y,n}^2$. (All summations are for h = 0, 1, 2, ..., N, and ν = N + 1.) The extent to which the variance of x is reduced by use of an m-term polynomial is

$$s_x^2 - s_{x,m}^2 = \nu^{-1} \sum x_{h,m} (x_{h,m} - 2x_h) - (\bar{x})^2. \tag{4.3}$$

Of greater interest than this absolute reduction in variance is the relative reduction, or squared correlation (sometimes called the coefficient of determination):

$$r^2_{x,m} = \frac{s^2_x - s^2_{x,m}}{s^2_x} = \frac{\sum x_{h,m}\,(x_{h,m} - 2x_h) - \nu(\bar{x})^2}{\sum x_h^2 - \nu(\bar{x})^2} . \qquad (4.4)$$

Similar expressions yield the absolute and relative reductions in the variance of y.

As more and more polynomial terms are used, i.e., as m and n increase, the variance reduction increases and the correlations approach one, attaining this value for $m = \nu = n$. But when $r^2 = .9$, the fit of the polynomial to the observations is considered adequate for most purposes, although in some cases values as high as .95 are desired.

However, the various terms of the polynomials may not be equally effective in reducing the variance. A higher power, such as a_4h^4, may be more effective than a lower one. Hence, the terms should be chosen not in simple order, but according to the amount of variance reduction that they provide.

A more efficient polynomial, in the sense of having fewer terms, would be formed from those terms, regardless of their exponents, providing the greatest reduction in variance, or highest correlation. The various terms, a_kh^k, should be arranged according to their contribution to the variance reduction. Coefficients ordered in this way may be denoted as $a_{(k)}h^{(k)}$, and the first m of them will be considered to form the index set M.

In this notation, the polynomial providing the required (e.g., 90%) relative reduction in variance is

$$x_{h,M} = \sum_{(k)=1}^{m} a_{(k)}h^{(k)} = \sum_{k\in M} a_k h^k, \qquad (4.5)$$

and similarly for $y_{h,N}$.

Such polynomials would provide suitably efficient procedures for representing each of the components separately. But they offer no link between the components; they do not apply to the wind vector itself. When results obtained by two such polynomials are combined to provide estimates of the wind vector at each level, excessive interlevel shears could be indicated. Hence, they do not seem particularly suited for the mathematical representation of wind vectors.

The same objections apply to the fitting of a complex variable by a single power series with complex coefficients:

$$\zeta_{h,M} = \sum_{k\epsilon M} c_k h^k = \sum_{k\epsilon M} (a_k + i\, b_k)\, h^k = \sum_{k\epsilon M} a_k h^k + i \sum_{k\epsilon M} b_k h^k. \qquad (4.4)$$

These objections to expressing the wind components as polynomial functions of height apply regardless of the method of estimating the polynomial coefficients. Orthogonal polynomials, while possessing the great advantage that they need not be recomputed after selection of the highest-order term contributing significantly to the variance reduction, are no better in these respects than simple power series.

5. Fourier

Complex trigonometric polynomials (Fourier series) are not subject to the same drawbacks as univariate polynomials, just discussed. The estimation of the coefficients of each component (i.e., the real and imaginary parts) is based on both components of the observed wind, and hence such a complex series actually estimates the vector, or entire complex number, rather than separate components.

Fourier series often are used to represent functions known to be periodic, but are not restricted to such use. Lighthill (1960) [3] declares (p.4) that a common application is "to represent a function which is not periodic, but instead is defined in the first place only in a restricted interval," covering perhaps 30 km in the vertical. Wind information usually is available only for a restricted interval. Description of the time and space variations in such a 30-km profile may be possible through the fitting of Fourier series or polynomials.

Such polynomials, however, have no linear terms. Since the wind often increases rather regularly with height, at least over certain height ranges, a linear term obviously is desirable in any expression for the vertical wind profile. This can be provided by defining a plane about which the actual wind observations vary, and then describing such

variations by Fourier polynomials. The required plane is defined by two intersecting straight lines, in the vertical x, h and y, h planes, respectively, that represent the individual wind components.

The original observations of the wind at level h,

$$\zeta_h = x_h + i\, y_h = z_h \exp(i\phi), \tag{5.1}$$

may be expressed in terms of the least squares linear trends as

$$\zeta_h = c_z + d_{oo} h + \eta_h. \tag{5.2}$$

The departure

$$\eta_h = u_h + i\, v_h$$

is given by

$$u_h = x_h - c_x - a_{oo}\, h, \qquad v_h = y_h - c_y - b_{oo} h. \tag{5.3}$$

The linear coefficients - reasons for the double zero subscripts will be apparent later - are

$$a_{oo} = \frac{\nu \sum x_h\, h - \sum x_h \sum h}{\nu \sum (h - \bar{h})^2}, \qquad b_{oo} = \frac{\nu \sum y_h\, h - \sum y_h \sum h}{\nu \sum (h - \bar{h})^2}. \tag{5.4}$$

The constant terms are

$$c_x = \bar{x} - a_{oo}\bar{h}, \qquad c_y = \bar{y} - b_{oo}\bar{h}. \tag{5.5}$$

Thus, the variations of the wind vector about the least squares plane are

$$\eta_h = \zeta_h - (\bar{\zeta} - d_{oo}\bar{h}) - d_{oo}h, \tag{5.6}$$

where $d_{oo} = a_{oo} + i\, b_{oo}$ is obtained from (5.4).

Fourier polynomials describing η_h are

$$\eta_{h,M} = \sum_{j\in M} d_j \exp(i\lambda jh), \quad \lambda = 2\pi/\nu. \tag{5.7}$$

The complex coefficients $d_j = a_j + i\, b_j$ are estimated (as explained in Appendix A, and discussed in the next section) from the ν values of η_h, obtained from the ν observations of ζ_h. Summation is over the set M of the m terms contributing most to the reduction in variance, as discussed in the previous section for univariate polynomials.

After the $\{d_j\}$ have been estimated and the set M chosen, the resulting Fourier polynomial can be augmented by the constant and linear terms to provide a complete expression for the actual wind profile:

$$\zeta_{h,M} = \bar{\zeta} + d_{oo}(h - \bar{h}) + \sum_{j\in M} d_j \exp(i\lambda jh). \tag{5.8}$$

Application of this expression for the wind profile to actual wind observations is discussed in the following sections.

6. Properties

Expansion of (5.7) shows that the estimation of each component of the wind vector $\eta_{h,M}$ and hence of $\zeta_{h,M}$, involves coefficients from both the real and imaginary parts of the polynomial:

$$\eta_{h,M} = \sum_{j\in M} (a_j + i\, b_j)(\cos\lambda jh + i \sin\lambda jh) = \sum_{j\in M} (a_j \cos\lambda jh - b_j \sin\lambda jh)$$

$$+ i \sum_{j\in M} (b_j \cos\lambda jh + a_j \sin\lambda jh). \tag{6.1}$$

The least squares estimators of the complex coefficients d_j are, as shown in Appendix A,

$$d_j = a_j + i\, b_j = \frac{1}{\nu} \sum_{h=0}^{N} \eta_h \exp(-i\lambda jh)$$

$$= \frac{1}{\nu} \sum_{h=0}^{N} (u_h + i\, y_h)(\cos \lambda jh - i \sin \lambda jh) \qquad (6.2)$$

$$= \frac{1}{\nu} \sum_{h=0}^{N} (u_h \cos \lambda jh + v_h \sin \lambda jh) + i \frac{1}{\nu} \sum_{h=0}^{N} (v_h \cos \lambda jh - u_h \sin \lambda jh).$$

That these estimators actually minimize the sum of the squared departures of the observations from the least-squares regression plane is shown in Appendix A. These squared departures are the sums of the squared departures of the two components; divided by ν, the total number of observations, they yield the conditional variance about the polynomial:

$$\frac{1}{\nu} \sigma^2_{\eta;M} = S^2_{\eta;M} = \sum_{h=0}^{N} S^2_{\eta,h;M} = \sum_{h=0}^{N} (\eta_h - \eta_{h;M})(\eta_h - \eta_{h;M})^* . \qquad (6.3)$$

A major purpose of this study is to determine the magnitude of the absolute reduction in variance, $\sigma^2_\eta - \sigma^2_{\eta;M}$ and the relative reduction, $r^2_{\eta;M}$ (4.4), when a wind profile, from which ν observations are obtained at equal height intervals, is approximated by (5.8) for $m \leq 4$. If the representation is adequate, $\zeta_{h;M}$ may be evaluated for any value of h, not necessarily those equally-spaced values at which ζ_h was observed. This would provide a continuous representation of a wind profile originally described for discrete points only.

In addition, the function (5.8) can be differentiated to provide a continuous representation of the wind shear, $\partial\zeta_{h;M}/\partial_h$. Alternatively, the ζ_h may be the balloon positions at successive heights, and differentiation then will provide wind speeds at any height.

Not only do the coefficients $\{d_j\}$, estimated by (6.2), minimize $S^2_{\eta;M}$, but, as discussed in Appendix B, they seem to be approximately orthogonal, although the precise extent of any slight dependence between them is still to be determined.

Orthogonality insures that for any set $\{M\}$ of coefficients,

$$S^2_{\eta,M} = \sum S^2_{\eta,j},$$

that is, that the contribution of each term to the total variance does not depend on what other terms are included in that total. This desirable property has been assumed in the preliminary applications of Fourier polynomials to the description of wind profiles.

Orthogonality properties are increased when the original observations ζ_h, expressed as departures η_h from the least-squares plane, all have the same variance. Thus, rather than η_h as defined by (5.6), computations of d_j by (6.2) should use $\eta_h/\sigma_{\eta;h}$, where $\sigma^2_{\eta;h}$ is the variance η_h. Since η_h is, by (5.6), a linear function of ζ_h, their variances are the same. Such variances should be used, when available, to adjust the values of η_h, as just indicated.

When the original observations $\zeta_h = x_h + i\, y_h$ are means, as for a month or season, variances are available for such adjustment. But when they are single observations, the proper choice of values is not obvious. In the following sections, examples are given of profiles computed from mean values adjusted for variance, and of profiles fitted to individual sets of observations without variance adjustment. The propriety of this second procedure, although it seems to provide an adequate fit, requires further investigation.

Another topic for further study is the method of computing the plane about which the departures η_h are taken. The Fourier polynomials may provide an even better approximation to the observations if this trend plane is constructed through the mean point so that the first and last observations (lowest and highest wind observations) are equidistant from it.

7. Applications

Augmented Fourier polynomials, as developed in the preceding two sections, were fitted to two sets of wind data to determine whether the method showed sufficient promise to warrant further study and development. Results of such application, presented in this section, are quite encouraging.

One set of wind data was composed of monthly mean winds, at 1-km levels, over Cape Kennedy, Florida. They are based on 5 years of observations (the first 321 days were at nearby Patrick Air Force Base), 1956-1961. Missing observations had been interpolated before averaging, so that sample sizes were the same at all levels. These data were furnished by Mr. Orvel E. Smith of the Aero-Astrodynamics Laboratory, George C. Marshall Space Flight Center, in advance of publication.

The other set was made up of four consecutive observations, at 6-hour intervals, over Montgomery, Alabama, on 9 January 1956. These were the first four consecutive soundings, each reaching to at least 25 km, in an extensive compilation of winter and summer soundings furnished by the National Weather Records Center, U. S. Weather Bureau, at Mr. Smith's request. These soundings also contained data on atmospheric density, so that momentum density as well as wind speed could be fitted by augmented Fourier polynomials. (Units of momentum density, the product of wind speed and atmospheric density, are dynes per cubic centimeter.)

These two sets of data provided a total of 20 "soundings," each sounding being a set of values of ζ_h for successive values of h. Of these, 12 were monthly means for Cape Kennedy, four were successive wind observations at Montgomery, and four were the corresponding momentum density observations. For each such "sounding," the lowermost 2 km were ignored, because of possible friction layer effects, as discussed in Section 3, and only the levels from 2 to 25 km, inclusive, were used. In the notation already developed, $h_0 = 2$ km, $h_1 = 3$ km, ..., $h_N = 25$ km.

Results of the fitting of the augmented Fourier polynomials to these 20 soundings are given in Tables 1 and 2. After the constant and linear terms, the coefficients are presented in decreasing order of the amount of variance "explained" by them. That is, the coefficients d_j have been ordered as $d_{(j)}$, as discussed in Section 4. For example, in the first line of Table 1 (for January mean winds over Cape Kennedy), $a_{(1)}$ and $b_{(1)}$ are, respectively, a_{23} and b_{23}, so that $j = 23$ is used in the trigonometric terms that they multiply.

Coefficients are given in Tables 1 and 2 for each wind component separately, as indicated in the formulas at the head of Table 2, which are based on (5.8) and (6.1). The two formulas may be combined into one expression, in complex notation. Thus, the mean January wind over Cape Kennedy may be written as

$$\zeta^{s}_{h,M} = (2.61 + 0.126\ i) - (0.054 - 0.003\ i)\ h$$

$$- (0.575 - 0.014\ i) \cos 23\pi\ h/12 - (0.014 + 0.575\ i) \sin 23\pi\ h/12$$

$$- (0.530 + 0.100\ i) \cos \pi\ h/12 + (0.100 - 0.530\ i) \sin \pi\ h/12$$

$$+ (0.044 + 0.173\ i) \cos 22\pi\ h/12 - (0.173 - 0.44\ i) \sin 22\pi\ h/12$$

$$+ (0.043 - 0.140\ i) \cos 2\pi\ h/12 + (0.140 + 0.043\ i) \sin 2\pi\ h/12. \qquad (7.1)$$

The superscript "s" indicates that the values of $\zeta^{s}_{h,M}$ obtained from (7.1), and from Table 1 generally, are for "standardized" values. They must be multiplied by the standard deviations of the wind components for the appropriate level to give values approximating the observed means.

For example, evaluation of (7.1) for h = 10, i.e., 12 km, gives 2.41 + 0.226 i. When each of these values is multiplied by the standard deviation of the corresponding wind component at 12 km over Cape Kennedy in January, 16.04 and 14.24 m/sec, respectively, estimated wind speeds are obtained which may be compared with the observed means:

Estimated	$x_{10} = 38.66$	$y_{10} = 3.22$
Observed	44.04	3.26.

In Figure 2, five hodographs are shown for the mean January winds over Cape Kennedy. In the upper panel, one hodograph depicts the actual means, in meters per second, while a second one shows the effect of dividing the speed at each level by its standard deviation, and expressing the result as a departure from the least-squares plane. The "trend" hodograph is centered at the origin, and is in units much smaller than those of the original values.

The lower panel of Figure 2 shows three hodographs, computed by Fourier polynomials, not augmented, i.e., as variations about the least-squares plane. The "one-term" hodograph is a circle, representing only the j = 23 term, without the preceding constant and linear terms or the

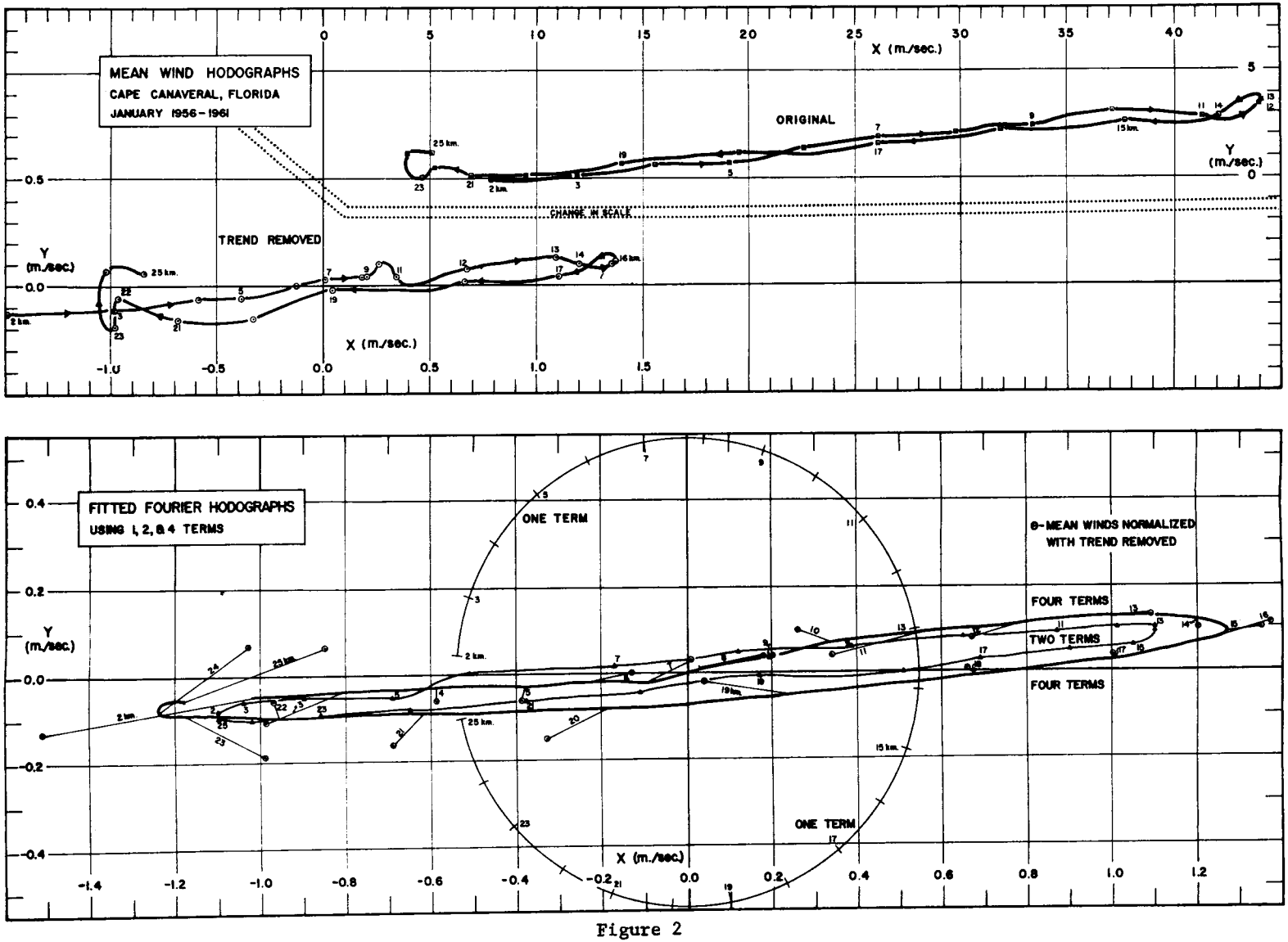
MEAN WIND HODOGRAPHS
CAPE CANAVERAL, FLORIDA
JANUARY 1956 - 1961
ORIGINAL
TREND REMOVED
CHANGE IN SCALE
X (m./sec.)
Y (m./sec.)
FITTED FOURIER HODOGRAPHS
USING 1, 2, & 4 TERMS
ONE TERM
FOUR TERMS
TWO TERMS
FOUR TERMS
ONE TERM
θ-MEAN WINDS NORMALIZED
WITH TREND REMOVED

Figure 2

final three terms. The "two-term" hodograph represents computation of the j = 23 and j = 1 terms in (7.1), without the constant and linear terms or the final two terms. The "four-term" hodograph presents results of using all terms of (7.1) except the constant and linear.

Shown as dots in the lower panel of Figure 2 are the same points, for each 1-km level, as in the "trend removed" hodograph of actual winds in the upper panel. The thin lines from these dots to the "four-term" curve indicate the extent of the vector difference between the observed mean winds, at each level, and the values computed from (7.1). The sum of the squares of the lengths of these thin lines is the $S^2_{\eta,M}$ of (6.3), for M = 4.

For the individual soundings over Montgomery, no estimates of wind variance at each level were readily available. The observed values were assumed to have the same variance, and no adjustments were made. Thus, the coefficients in Table 2, when introduced into the appropriate formula, give estimated winds directly in meters per second.

8. Discussion

Under each pair of coefficients in Tables 1 and 2 are two additional entries: the value of the index j for the pair, and the value of r^2, the relative reduction in variance (4.4) attained by using that term, and all preceding ones, in the augmented Fourier polynomial.

For the Cape Kennedy mean monthly wind profiles, the constant and linear terms alone reduce the variance by 80 percent in summer, but hardly at all in November and December. Two additional terms provide r^2 of 85 percent or more in all months, indicating that augmented Fourier polynomials of as few as four terms (m = 2) may provide descriptions adequate for some purposes. In nine of the months, term 23 provides the greatest reduction in variance, followed by term 1, while the same terms appear in reverse order in the other three months.

For all four Montgomery 6-hourly soundings, term 1 contributes most to the reduction in variance for both wind speed and momentum density. But whereas term 23 is second most important for wind speed, terms 2 (once) and 22 (thrice) have this role for momentum density. Values of r^2 for momentum density are consistently higher than for wind speed alone. Most of this difference arises in the constant and linear terms, for which r^2 is between 75 and 86 percent for momentum density, but only from 39 to 44 percent for wind speed. This may be a reflection of "Egnell's law," outlined in Section 3, and requires further study.

The extent to which these results depend on the particular height interval chosen also requires additional investigation. The strongest wind speeds in all the soundings are near the middle of the 2 to 26 km interval studied, which may explain the consistent appearance of term 1 as contributing significantly to the relative reduction in variance. Similarly, the importance of term 23 may indicate excessive level-to-level variability, perhaps actual but also possibly arising from observational errors and computational procedures in the compilation of wind information.

These and other considerations indicate that the most fruitful application of augmented Fourier polynomials to wind profile description may be their use to describe the position hodograph, as obtained directly from a balloon or other indicator, and the subsequent differentiation of the polynomial to provide wind speeds. This may provide considerable improvement over the present method employing successive finite differences, and may give greater detail of the wind profile and of its derivative, the wind shear.

Other topics for further study are statistical tests for the similarity or differences of two wind profiles, leading to criteria for their combination. For example, are January and February wind profiles over Cape Kennedy sufficiently similar that a combined winter profile describes them adequately? Also requiring study are procedures for predicting one profile from another, as in the case of the 6-hourly soundings over Montgomery.

Despite the need for these various extensions of the study, and further elaboration of the technique, the work reported here shows that mathematical description of an entire wind profile, either means or "instantaneous," can be attained with acceptable precision by the use of augmented Fourier polynomials.

TABLE 1. COEFFICIENTS OF AUGMENTED FOURIER POLYNOMIALS, AND CUMULATIVE REDUCTION IN RELATIVE VARIANCE, r^2, FOR MEAN MONTHLY WINDS OVER CAPE KENNEDY, FLORIDA, 1956-1961

	c_x c_y	a_{oo} b_{oo}	$a_{(1)}$ $b_{(1)}$	$a_{(2)}$ $b_{(2)}$	$a_{(3)}$ $b_{(3)}$	$a_{(4)}$ $b_{(4)}$
JAN	2.61 0.126 j=00	-0.054 0.003 r^2=16.5	-0.575 0.014 j=23 r^2=55.6	-0.530 -0.100 j=1 r^2=90.0	0.044 0.173 j=22 r^2=93.7	0.043 -0.140 j=2 r^2=96.2
FEB	2.11 0.409 j=00	-0.048 -0.017 r^2=17.2	-0.505 -0.039 j=23 r^2=53.1	-0.492 -0.073 j=1 r^2=87.8	0.041 0.181 j=22 r^2=92.6	0.077 -0.168 j=2 r^2=97.4
MAR	2.90 0.320 j=00	-0.086 -0.014 r^2=26.1	-0.695 -0.173 j=1 r^2=62.8	-0.675 0.052 j=23 r^2=95.7	0.074 -0.103 j=2 r^2=96.9	-0.057 0.085 j=3 r^2=97.6
APR	1.69 -0.055 j=00	-0.056 -0.010 r^2=19.9	-0.548 0.007 j=1 r^2=58.5	-0.509 0.091 j=23 r^2=92.9	0.050 -0.138 j=2 r^2=95.7	0.046 0.128 j=22 r^2=98.1
MAY	1.43 0.190 j=00	-0.098 -0.022 r^2=38.4	-0.642 0.050 j=23 r^2=71.5	-0.540 -0.034 j=1 r^2=94.8	0.101 0.155 j=22 r^2=97.5	-0.037 -0.132 j=2 r^2=99.0
JUN	1.67 -0.035 j=00	-0.202 -0.021 r^2=70.1	-0.610 0.234 j=23 r^2=85.2	-0.584 0.104 j=1 r^2=97.7	0.149 -0.080 j=1 r^2=98.7	-0.021 -0.121 j=2 r^2=99.2
JUL	1.41 0.298 j=00	-0.277 -0.036 r^2=84.0	-0.513 0.282 j=23 r^2=91.7	-0.545 0.097 j=1 r^2=98.6	0.120 -0.001 j=22 r^2=98.9	0.073 -0.062 j=2 r^2=99.1
AUG	1.46 0.208 j=00	-0.263 -0.023 r^2=79.8	-0.579 0.237 j=23 r^2=89.2	-0.589 -0.026 j=1 r^2=97.5	0.170 0.029 j=22 r^2=98.2	0.149 -0.042 j=2 r^2=98.8
SEP	1.06 0.174 j=00	-0.157 -0.018 r^2=62.0	-0.584 0.139 j=23 r^2=80.7	-0.558 -0.108 j=1 r^2=97.4	0.093 -0.012 j=22 r^2=97.9	0.058 -0.063 j=2 r^2=98.3
OCT	1.43 0.064 j=00	-0.075 -0.013 r^2=38.9	-0.435 0.153 j=23 r^2=69.0	-0.420 -0.079 j=1 r^2=94.8	-0.043 -0.083 j=21 r^2=96.0	-0.033 0.079 j=3 r^2=97.0
NOV	1.29 -0.064 j=00	-0.011 0.000 r^2=2.2	-0.332 0.113 j=23 r^2=47.9	-0.325 -0.067 j=1 r^2=88.8	-0.043 0.078 j=3 r^2=91.7	-0.022 -0.060 j=21 r^2=93.2
DEC	1.63 0.234 j=00	0.009 0.002 r^2=1.2	-0.366 -0.104 j=1 r^2=43.8	-0.372 0.027 j=23 r^2=84.7	0.054 -0.090 j=2 r^2=87.9	0.008 0.098 j=22 r^2=90.8

TABLE 2. COEFFICIENTS OF AUGMENTED FOURIER POLYNOMIALS, AND CUMULATIVE REDUCTION IN RELATIVE VARIANCE, r^2, FOR WIND SPEED AND MOMENTUM DENSITY OVER MONTGOMERY, ALABAMA, 9-10 JANUARY 1956

Wind components, x_h and y_h, at height h (in km starting at 2 km MSL), where $H = \pi h/12$, given by:

$$x_h = (c_x + a_{oo}h) + (a_{(1)} \cos j_1H - b_{(1)} \sin j_1H) + (a_{(2)} \cos j_2H - b_{(2)} \sin j_2H) + (a_{(3)} \cos j_3H - b_{(3)} \sin j_3H) + \ldots$$

$$y_h = (c_y + b_{oo}h) + (a_{(1)} \sin j_1H + b_{(1)} \cos j_1H) + (a_{(2)} \sin j_2H + b_{(2)} \cos j_2H) + (a_{(3)} \sin j_3H + b_{(3)} \cos j_3H) + \ldots$$

HOUR	c_x c_y	a_{oo} b_{oo}	$a_{(1)}$ $b_{(1)}$	$a_{(2)}$ $b_{(2)}$	$a_{(3)}$ $b_{(3)}$	$a_{(4)}$ $b_{(4)}$
			Wind Speeds			
0900	29.04 -33.62 j=00	-1.046 1.365 r^2=44.1	-8.852 -3.035 j=1 r^2=71.4	-5.542 3.716 j=23 r^2=85.3	-0.016 -3.253 j=22 r^2=88.6	0.079 2.779 j=2 r^2=91.0
1500	22.95 -27.52 j=00	-0.903 1.050 r^2=38.6	-7.843 -0.571 j=1 r^2=67.6	-4.743 4.604 j=23 r^2=82.9	-2.465 -0.154 j=22 r^2=85.5	1.260 1.808 j=2 r^2=87.5
2100	26.46 -26.42 j=00	-1.016 1.052 r^2=41.3	-8.115 -1.507 j=1 r^2=68.8	-6.021 3.499 j=23 r^2=88.4	1.840 2.610 j=2 r^2=92.5	-1.681 0.566 j=17 r^2=93.8
0300	28.42 -22.88 j=00	-1.146 0.913 r^2=42.9	-7.428 -1.161 j=1 r^2=66.5	-3.612 4.576 j=23 r^2=80.7	2.872 1.630 j=2 r^2=85.3	-0.697 -2.806 j=22 r^2=88.8
			Momentum Density			
0900	15.14 -22.92 j=00	-0.705 1.231 r^2=80.3	-1.036 -3.499 j=1 r^2=91.4	-0.943 1.357 j=2 r^2=93.7	-0.504 -1.321 j=22 r^2=95.4	-0.957 -0.687 j=23 r^2=96.6
1500	11.16 -17.63 j=00	-0.509 0.916 r^2=74.4	-1.293 -2.339 j=1 r^2=84.5	-1.572 -0.409 j=22 r^2=88.2	-0.832 -0.750 j=19 r^2=90.0	-0.663 0.630 j=3 r^2=91.2
2100	13.57 -17.71 j=00	-0.638 0.942 r^2=83.4	-0.826 -2.474 j=1 r^2=92.5	-0.505 -0.776 j=22 r^2=93.7	0.092 0.914 j=2 r^2=94.8	-0.800 -0.363 j=23 r^2=95.8
0300	15.70 -14.69 j=00	-0.773 0.768 r^2=86.3	-0.543 -1.739 j=1 r^2=91.3	-0.939 -0.720 j=22 r^2=93.4	-0.894 -0.717 j=21 r^2=95.4	0.284 0.839 j=2 r^2=96.6

APPENDIX A

ESTIMATION OF COEFFICIENTS

Complex coefficients $d_j = a_j + i\, b_j$, for $j = 0, 1, \ldots, N$, are to be estimated from a set of $\nu = N + 1$ complex numbers η_h so as to minimize the sum of the squared differences

$$S^2_{\eta;M} = \sum_{h=0}^{N} S^2_{\eta;h,M} = \sum_{h=0}^{N} (\eta_h - \eta_{h;M})\ (\eta_h - \eta_{h;M})^* \qquad \text{(A-1)}$$

for each index set M containing $1 \leqq m \leqq \nu$ elements, when the estimators $\eta_{h;M}$ are obtained from

$$\eta_{h;M} = \sum_{j \in M} d_j \exp\ (i\lambda\ jh), \qquad \lambda = 2\pi/\nu. \qquad \text{(A-2)}$$

The ν numbers $\{\eta_h\}$ are assumed to represent values or observations at ν equal intervals $h = 0, 1, \ldots, N$. These may be intervals of time or space; in the specific applications to be made here, they are equal intervals of height, and the numbers $\{\eta_h\}$ represent wind vectors at successive levels in the atmosphere. These vectors are expressed as departures from a plane of best fit, in the sense of minimizing variance, to the basic data; that is, any linear trend with height has been removed.

For each value of h

$$S^2_{\eta;h,M} = (\eta_h - \eta_{h;M})\ (\eta^*_h - \eta^*_{h;M})$$

$$= \left(\eta_h - \sum_M d_j\ e^{i\lambda jh}\right)\left(\eta^*_h - \sum_M d^*_j\ e^{-i\lambda\ jh}\right) \qquad \text{(A-3)}$$

$$= w^2_h + \left|\sum_M d_j\ e^{i\lambda\ jh}\right|^2 - 2\tilde{\tilde{R}}\left(\eta_h \sum_M d^*_j\ e^{-i\lambda\ jh}\right)$$

---

* The asterisk, *, denotes the complex conjugate.

because $\eta_h \eta_h^* = |\eta_h|^2 = w_h^2$, in the notation of Section 1. Since $\exp [i\lambda h(j - k)] = 1$ when $j = k$, the second term becomes

$$\left| \sum_{j \in M} d_j \, e^{i\lambda jh} \right|^2 = \sum_{j \in M} \sum_{k \in M} d_j \, d_k^* \, e^{i\lambda h(j-k)}$$

$$= \sum_{j \in M} |d_j|^2 + \sum_{j \neq k} \sum d_j \, d_k^* \, e^{i\lambda h(j-k)}. \qquad \text{(A-4)}$$

Expression of $\eta_h \exp (- i\lambda jh)$ as $\alpha_{hj} + i\beta_{hj}$ permits the final term in (A-3) to be written as

$$\eta_h \sum_{j \in M} d_j^* \, e^{-i\lambda jh} = \sum_{j \in M} d_j \, \eta_h \, e^{-i\lambda jh}$$

$$= \sum_{j \in M} (a_j - i \, b_j) \, (\alpha_{hj} + i\beta_{hj}). \qquad \text{(A-5)}$$

Since $|d_j|^2 = a_j^2 + b_j^2$ and $\Sigma \exp [i\lambda h(j - k)] = 0$, the sum of squares (A-1) to be minimized becomes

$$S^2_{\eta;M} = \sum_{h=0}^{N} S^2_{\eta;h,M} = \sum_{h=0}^{N} w_h^2 + \nu \sum_{j \in M} (a_j^2 + b_j^2)$$

$$- 2 \sum_{h=0} \sum_{j \in M} (a_j \, \alpha_{hj} + b_j \, \beta_{hj}). \qquad \text{(A-6)}$$

The usual minimization procedures give, for each value of j,

$$\frac{\partial S^2_{\eta;M}}{\partial a_j} = 2\nu\, a_j - 2 \sum_{h=0}^{N} \alpha_{hj},$$

$$\frac{S^2_{\eta;M}}{\partial b_j} = 2\nu\, b_j - 2 \sum_{h=0}^{N} \beta_{hj}. \qquad \text{(A-7)}$$

Setting these derivatives equal to zero gives

$$a_j = \frac{1}{\nu} \sum_{h=0}^{N} \alpha_{hj}, \qquad b_j = \frac{1}{\nu} \sum_{h=0}^{N} \beta_{hj}. \qquad \text{(A-8)}$$

Consequently,

$$d_j = \frac{1}{\nu} \sum_{h=0}^{N} (\alpha_{hj} + i\, \beta_{hj}) = \frac{1}{\nu} \sum_{h=0}^{N} \eta_h \exp(-i\lambda jh). \qquad \text{(A-9)}$$

For computation, the real and imaginary parts are evaluated separately:

$$a_j = \frac{1}{\nu} \sum_{h=0}^{N} [u_h \cos(\lambda jh) + v_h \sin(\lambda jh)],$$

$$b_j = \frac{1}{\nu} \sum_{h=0}^{N} [v_h \cos(\lambda jh) - u_h \sin(\lambda jh)]. \qquad \text{(A-10)}$$

In polar coordinates,

$$a_j = \frac{1}{\nu} \sum_{h=0}^{N} w_h \cos (\xi_h - \lambda jh),$$

$$b_j = \frac{1}{\nu} \sum_{h=0}^{N} w_h \sin (\xi_h - \lambda jh). \qquad \text{(A-11)}$$

Use in (A-2) of any set of m of these values for $d_j = a_j + i\, b_j$ will insure that the resulting estimator, $\eta_{h;M}$, when introduced into (A-1), will minimize the sum of squares $S^2_{\eta;M}$. When $m = \nu$, i.e., when the sum (polynomial) has as many terms as the original observations, $S^2_{\eta;M} = 0$. For smaller sets, i.e., for $m < \nu$, the sum of squares $S^2_{\eta;M}$ will depend on the exact composition of the set M. Thus, $S^2_{\eta;M}$ can be computed for each of the ν sets M in which m = 1, i.e., for one term only, and for the $\nu(\nu + 1)/2$ sets of two terms each, and so on, to find the combination giving an acceptably small $S^2_{\eta;M}$ from the smallest set M.

However, when the coefficients $\{d_j\}$ are orthogonal, in the statistical sense, the contribution of each is independent of that of the others, and

$$S^2_{\eta;M} = \sum_{j \in M} S^2_{\eta;j}. \qquad \text{(A-12)}$$

Then, $S^2_{\eta;j}$ can be computed for each orthogonal d_j and ranked in descending order to determine the minimum set M for which $S^2_{\eta;M}$ is acceptably small. The extent to which the coefficients $\{d_j\}$, estimated by (A-9), (A-10), or (A-11), satisfy these requirements is examined in Appendix B.

APPENDIX B

ORTHOGONALITY

Two different kinds of orthogonality are involved in the development of complex Fourier polynomials for the respresentation of wind profiles. One kind is that of the series of orthogonal polynomials used to represent a sounding. In such representation, functional orthogonality requires that

$$\sum e^{i\lambda\, jh_e\; i\lambda\, kh} = \begin{cases} \nu, & j = k \\ 0, & j = k. \end{cases}$$

Use of such a system of orthogonal functions permits judgement of the adequacy of the representation in terms of the sum of the squares of the coefficients. This sum measures the sum of the squares of the differences between the polynomial representation and the function being fitted, after removal of linear trend. When orthogonal functions are used, a smaller number of terms can be selected without recomputation of coefficients.

Another kind of orthogonality appears when a sounding is viewed as a collection of random variables. Then the coefficients $\{d_j\}$ in the Fourier representation (5.7) are also random variables, since they are linear combinations of the original random variables (6.2). Orthogonality of the system of coefficients $\{d_j\}$ is tantamount to their being uncorrelated. Uncorrelated Gaussian random variables are statistically independent - a very highly desirable property in computing probability statements. The basic physical quantities, i.e., balloon displacements or wind speeds, expressed in cartesian coordinates, are usually assumed to be approximately Gaussian. Hence the coefficients $\{d_j\}$, being linear combinations of them, also should be approximately Gaussian, especially because of central limit effects.

Orthogonality of the $\{d_j\}$ is almost impossible to establish unless the $\{\eta_h\}$ are second-order stationary with a real covariance function. The need for second-order stationarity, that is, that the covariance of (η_h, η_ℓ) depend only on the difference $|h - \ell|$, appears in the evaluation of the expression for the variances of the individual d_j. When the expectations of the $\{\eta_h\}$, and hence of the $\{d_j\}$, are zero, the variance of each d_j is given by

$$E(d_j\, d_j^*) = \nu^{-2} \sum_{h=0}^{N} \sum_{\ell=0}^{N} \exp\,[i\lambda\, j(\ell - h)]\; E(\eta_h\, \eta_\ell^*). \qquad \text{(B-1)}$$

* The asterisk, *, denotes the complex conjugate.

This involves the covariance of the observed values, or their departures from the plane, which in turn depends on the correlation (r) between the two components:

$$E(\eta_h\ \eta_\ell^*) = E\Big[(u_h u_\ell + v_h v_\ell) + i(u_\ell v_h - u_h v_\ell)\Big]$$

$$= \Big[r(u_h,u_\ell) + r(v_h,v_\ell)\Big] + i\Big[r(u_\ell,v_h) - r(u_h,v_\ell)\Big]\ . \tag{B-2}$$

Second-order stationarity requires that these correlations depend, for each variable u or v, and for any separation h - ℓ, denoted as τ, only on the separation:

$$r(u_h,\ u_\ell) = r_u(h - \ell) = r_u(\tau) = r_u(-\tau). \tag{B-3}$$

Certain properties of the separation τ are needed:

$$\tau = h\ - \ell, \qquad -N \leqq \tau \leqq +N,$$
$$\max\ (-\tau,\ 0) \leqq \ell \leqq \min\ (N - \tau,\ N). \tag{B-4}$$

In this notation, (B-2) becomes

$$E(\eta_h\ \eta_\ell^*) = \Big[r_u(\tau) + r_v(\tau)\Big] + i\Big[r_{uv}(-\tau) - r_{uv}(\tau)\Big] = C(\tau), \tag{B-4}$$

where C may be called a correlation function; $C(0) = 2$, because $r_u(0) = r_v(0) = 1$. In terms of this function C, the expression (B-1) for the variance is

$$E(d_j\ d_j^*) = \nu^{-2} \sum_{-N}^{+N} C(\tau)\ \exp\ (i\lambda\ j\tau)\ (\nu - \tau)$$

$$= \nu^{-1} \sum_{-N}^{+N} (1 - \tau/\nu)\ \cos\ (\lambda j\tau)\ \widetilde{\widetilde{R}}[C(\tau)] \tag{B-5}$$

$$= \nu^{-1} \left[C(0) + 2 \sum_{1}^{N} (1 - \tau/\nu)\ \cos\ (\lambda j\tau)\ \widetilde{\widetilde{R}}\ C(\tau)\right]$$

because the variance is real-valued. [All summations are over the range of τ given by (B-4).] Similarly, the covariance function for the coefficients is

$$E(d_j\, d_k^*) = \nu^{-2} \sum_{h=0}^{N} \sum_{\ell=0}^{N} \exp\left[i\lambda\,(k\ell - jh)\right] E(\eta_h\, \eta_\ell^*)$$

$$= \nu^{-2} \sum_{\tau=-N}^{N} C(\tau) \exp\,(-\,i\lambda\, j\tau) \sum_{\ell} \exp\,(i\lambda\, \ell p), \qquad (B\text{-}6)$$

$$p = k - j,$$

because $k\ell - jh = \ell p - j\tau$. This must be zero for d_j and d_k to be orthogonal. To determine whether such is the case, (B-6) must be examined term by term, invoking the orthogonality properties of trigonometric series.

Since

$$\sum_{j=0}^{m} r^j = \frac{1 - r^{m+1}}{1 - r},$$

$$\sum_{j=0}^{N} \exp\,(i\lambda\, jp) = \begin{cases} \dfrac{1 - [\exp\,(i\lambda p)]^{\nu}}{1 - [\exp\,(i\lambda p)]}, & p \neq 0, \\ N + 1 = \nu, & p = 0. \end{cases} \qquad (B\text{-}7)$$

The last summation in (B-6), over ℓ, is, by definition (B-4), from max $(-\tau, 0)$ to min $(N - \tau, N)$, and hence depends on τ as well as on p. It may be denoted as $\gamma(\tau, p)$:

$$\gamma(\tau, p) = \sum_{\ell} \exp\,(i\lambda\ell p) = \begin{cases} 0 & \begin{cases} \tau = 0, \\ 0 \leq \ell \leq N; \end{cases} \\ \dfrac{1 - \exp\,(-i\lambda\, p\tau)}{1 - \exp\,(i\lambda p)} & \begin{cases} \tau > 0, \\ 0 \leq \ell \leq N - \tau; \end{cases} \\ -\dfrac{1 - \exp\,(-i\lambda\, p\tau)}{1 - \exp\,(i\lambda p)} & \begin{cases} \tau < 0, \\ -\tau \leq \ell \leq N. \end{cases} \end{cases} \qquad (B\text{-}8)$$

Thus, $\gamma(-\tau, p) = -\gamma(\tau, p)$. In the expression for $\gamma(\tau, p)$ when $\tau > 0$, multiplication of numerator and denominator by $1 - \exp(-i\lambda p)$ gives

$$\gamma(\tau, p) = \frac{(1 - e^{i\lambda p})(1 - e^{-i\lambda p\tau})}{2 - 2\cos \lambda p} \qquad \tau > 0. \tag{B-9}$$

This is zero when $p\tau$ is an integral multiple of ν and is small for τ such that $p\tau$ is close to an integral multiple of ν.

Next, the correlation function $C(\tau)$ must be examined. It is real if and only if it is even, i.e., if $r_{uv}(-\tau) = r_{uv}(\tau)$. In this case, (B-6) becomes

$$\begin{aligned} E(d_j d_k^*) &= \frac{1}{\nu}\left\{ \sum_{\tau=1}^{N} C(\tau)\, e^{-i\lambda\tau j}\, [\gamma(\tau,p)/\nu] + \sum_{\tau=1}^{N} C(-\tau)\, e^{i\lambda\tau j}[-\gamma(\tau,p)/\nu]\right\} \\ &= \frac{1}{\nu}\left\{- \sum_{\tau=1}^{N} C(\tau)\, [\gamma(\tau,p)/\nu]\, [e^{i\lambda\tau j} - e^{-i\lambda\tau j}]\right\} \\ &= \frac{1}{\nu}\left\{- \sum_{\tau=1}^{N} C(\tau)\, [\gamma(\tau,p)/\nu]\, [2i \sin j\lambda\tau]\right\} \\ &= 0(\tfrac{1}{\nu}). \end{aligned} \tag{B-10}$$

The summand of equation (B-10) will not be large since $|C(\tau)| \leq C(0) = 2$ and tends to zero as τ becomes large. The multiplier $\sin i\lambda\tau$ will have a dampening effect for the smaller values of τ.

Thus, $E(d_j d_k^*)$ apparently is always small, although that it is identically zero for all τ, as is required for complete orthogonality, has not been proved. Actually, $E(d_j d_k^*) \to 0$ as $N + 1 = \to \infty$, i.e., as more and more levels are used and the discrete model approaches a continuous one. Thus, the question of orthogonality may be analogous to the general problem of the extent to which large sample theory can be used for small samples, or to which properties of a continuous function can be applied to a discrete one. For the present purpose, the assumption of orthogonality seems reasonable.

REFERENCES

1. Humphreys, W. J., Physics of the Air, McGraw Hill, 654 pp., 1929.

2. Hess, Seymour L., Introduction to Theoretical Meteorology, Henry Holt & Co., 362 pp., 1959.

3. Lighthill, M. J., "Fourier Analysis and Generalized Functions," Cambridge University Press, 79 pp., 1960.

DISTRIBUTION

Dep Dir Technical
Dr. Rees

R&D Operations
Mr. Weidner

Aero Laboratory
Dr. Geissler
Mr. O. C. Jean
Mr. R. Cummings
Mr. H. Horn
Mr. C. Baker
Dr. F. Speer
Mr. J. Lindberg
Mr. L. Stone
Mr. T. Reed
Mr. J. de Fries
Mr. L. McNair
Mr. W. W. Vaughan (5)
Mr. G. E. Daniels (25)

Mr. J. Kaufman
Mr. W. K. Dahm
Mr. O. E. Smith (50)
Mr. R. Ryan
Mr. J. Lovingood
Mr. D. Mourry
Mr. M. Rheinfurth
Mr. R. Lewis
Dr. R. Hoelker

P&VE Laboratory
Mr. E. Goerner
Mr. N. Showers
Mr. R. Hunt

ASTR Laboratory
Mr. H. Hosenthien
Mr. H. Mink
Mr. J. Blackstone

TEST Laboratory
Mr. K. Heimburg
Dr. W. Sieber

Industrial Operations

S-IB, Mr. L. James
S-V, Dr. Rudolph

MISS. TEST OPERATIONS
Mr. L. W. Nybo

Kennedy Space Center (NASA)
Cape Kennedy, Florida
Dr. K. Debus
Dr. Knothe (2)
Dr. H. Gruene
Col. R. Petrone
Mr. A. Taiani
Mr. J. Deese
Mr. G. von Tiesenhausen
Mrs. Russell, Technical Library

Army Missile Command
Redstone Arsenal, Alabama
Library
Dr. Essenwanger

Manned Spacecraft Center (NASA)
Cape Kennedy, Florida
Apollo Spacecraft Projects Office
Mr. Jerry Valek

Eastern Test Range
Patrick Air Force Base, Florida
Staff Meteorologist
Det. 11, 4th Weather Group

Pan American World Airways
Patrick Air Force Base, Florida
Division Meteorologist

Weather Bureau, U. S. Dept. of
Commerce, Washington, D. C.
Dr. R. M. White, Chief
Dr. H. E. Landsberg
Mr. K. Nagler
Dr. I. Van der Hoven

DISTRIBUTION CONT'D

National Weather Records Center
Asheville, North Carolina
Dr. Barger
Dr. Crutcher
Mr. Truppi

Langley Research Center (NASA)
Langley Field, Virginia
H. B. Tolefson (2)
Veronon Alley
Library

Wallops Island (NASA)
Wallops Island, Virginia
Mr. Spurling

Goddard Space Flight Center (NASA)
Greenbelt, Maryland
Mr. W. Stroud

NASA Headquarters
Washington, D. C.
Office of Advanced Research
& Technology

Mr. D. Gilstad, RV-2
Dr. A. Kelley, RE

Office of Space Sciences
& Application
Dr. M. Tepper
Dr. H. Newell

Office of Manned Space Flight
NASA Headquarters
Washington, D. C.
Gemini Program Director
Apollo Program Director
Advanced Mission Program
Director

Air Force Cambridge Research
Laboratories,
L. G. Hanscom Field
Bedford, Massachusetts
Mr. N. Sissenwine (2)
Dr. M. Barad
Technical Library

Manned Spacecraft Center (NASA)
Houston, Texas
Director
Apollo Project Office Director
Mr. Calvin Perrine
Mr. Donald Wade
Mr. Dallas Evans
Mr. John Mayer

Commander (2)
Air Weather Service
Scott Air Force Base, Illinois

Air Force System Command (2)
Code: SCWTS
Andrews Air Force Base
Washington, D. C. 20331

Mr. George Muller (2)
Air Force Flight Dynamic Laboratory
Air Force System Command
Wright Patterson Air Force Base, Ohio

Air Force Systems Command
Space System Division
Air Force Unit Post Office
Los Angeles 45, California

Meteorological & Geoastrophysical
Abstracts
P. O. Box 1736
Washington 13, D. C.

Mr. Richard Martin
General Dynamics Astronautics
San Diego, California

Mr. Carl Wentworth
NASA-Lewis Research Center
2100 Brookpark Road
Cleveland, Ohio

Mr. Robert Borland
Apollo Support Dept
General Electric Co.
P. O. Box 26287
Houston 32, Texas

DISTRIBUTION CONT'D

Mr. Marvin White
Space Technology Laboratories, Inc.
Structures Department
One Space Park
Redondo Beach, California

Scienfific & Technical Information
Facility (25)
Attn: NASA Representative (S-AK/-
P. O. Box 5700 RKT)
Bethesda, Maryland

Physical & Life Sciences Laboratory
Lockheed-California Company
Burbank, California

Dr. D. T. Perkins (25)

Dr. Robert R. Reed (10)
Department of Mathematics
U. S. Navy Postgraduate School
Monterey, California

Dr. H. Panofsky
Pennsylvania State University
Dept. of Meteorology
State College, Pennsylvania

Dr. Thomas Gleeson
Florida State University
Tallahassee, Florida

Dr. Elmer Reiter
Colorado State University
Fort Collins, Colorado

Mr. Jerry Bidwell
Martin Company
Denver, Colorado

Director
Meteorological Division
U. S. Army Signal Research &
Development Laboratories
Ft. Monmouth, New Jersey

Mr. Clyde Martin
North American Aviation
S&ID
Downey, California

Mr. Raymond Beiber
Lockheed Company
Research Park
Huntsville, Alabama

Dr. Arnold Court (50)
17168 Septo Street
Northridge, California

Dr. James R. Scoggins
605 Ethel Road
Bryan, Texas 77801